http://dx.doi.org/10.5012/bkcs.2013.34.2.519

Modified Shrinking Core Model for Atomic Layer Deposition of TiO_2 on Porous Alumina with Ultrahigh Aspect Ratio

Inhye Park,[a] Jina Leem,[a] Hoo-Yong Lee, and Yo-Sep Min[*]

Department of Chemical Engineering, Konkuk University, Seoul 143-701, Korea. [*]E-mail: ysmin@konkuk.ac.kr
Received October 23, 2012, Accepted November 19, 2012

When atomic layer deposition (ALD) is performed on a porous material by using an organometallic precursor, minimum exposure time of the precursor for complete coverage becomes much longer since the ALD is limited by Knudsen diffusion in the pores. In the previous report by Min *et al*. (Ref. 23), shrinking core model (SCM) was proposed to predict the minimum exposure time of diethylzinc for ZnO ALD on a porous cylindrical alumina monolith. According to the SCM, the minimum exposure time of the precursor is influenced by volumetric density of adsorption sites, effective diffusion coefficient, precursor concentration in gas phase and size of the porous monolith. Here we modify the SCM in order to consider undesirable adsorption of byproduct molecules. TiO_2 ALD was performed on the cylindrical alumina monolith by using titanium tetrachloride ($TiCl_4$) and water. We observed that the byproduct (*i.e.*, HCl) of TiO_2 ALD can chemically adsorb on adsorption sites, unlike the behavior of the byproduct (*i.e.*, ethane) of ZnO ALD. Consequently, the minimum exposure time of $TiCl_4$ (~16 min) was significantly much shorter than that (~ 71 min) of DEZ. The predicted minimum exposure time by the modified SCM well agrees with the observed time. In addition, the modified SCM gives an effective diffusion coefficient of $TiCl_4$ of ~1.78×10^{-2} cm^2/s in the porous alumina monolith.

Key Words : Shrinking core model, Atomic layer deposition, TiO_2, Porous alumina, Aspect ratio

Introduction

Atomic layer deposition (ALD) is one of chemical vapor deposition (CVD) methods, which is specially modified to obtain a conformal film *via self-limiting chemisorption*.[1-7] While in CVD a precursor vapor (*e.g.*, $TiCl_4$) is simultaneously supplied with a reaction gas (*e.g.*, H_2O) onto a substrate to grow a binary film (*e.g.*, TiO_2), in ALD the precursor and reaction gases are alternately pulsed, and their pulses are separated by purging steps by an inert gas. Thus in an ALD process for binary film, the typical sequence of ALD consists of precursor pulse - purge - reaction gas pulse - purge, and the sequence is repeated to grow a film with a required thickness. Consequently the binary film grows through chemisorption between the gaseous molecules (*i.e.*, precursor vapor or reactant gas) and reactive functional groups on the surface (*e.g.*, hydroxyl groups or chemisorbed organometallic groups). Once vacant adsorption sites become saturated by adsorbate molecules, the precursor or reactant gas in excess do not chemically adsorb to form any multilayer. Therefore if sufficient amounts of precursor vapor and reactant gases are supplied to the substrate, highly conformal growth can be achieved even on porous materials with ultrahigh aspect ratio (> 10^3).

ALD on porous materials has been intensively investigated because catalytically active elements can be formed on the porous materials in an atomically-controlled manner.[8,9] Recently, nano-materials such as nanotubes and nanoparticles have been also prepared by using the conformality of ALD.[10-12] However, for the conformal deposition on porous materials, the exposure time of precursor molecules should be much longer comparing with the exposure time on a flat substrate, because the chemisorption of the precursor is limited by the Knudsen diffusion on the internal surface of the porous materials.[13-21] In smaller pores with a longer depth, it is more difficult for the precursor to reach vacant sites which locate at the core of the porous materials. In addition, the number of adsorption sites in the porous materials is much higher than that in the flat substrate, due to their high specific surface area.

Several groups suggested theoretical models to predict the minimum exposure time of precursor for the conformal growth.[13,14,22] In their models they assume the pores (or holes) to be deposited are straight, however the pores in typical porous materials are rather tortuous. Recently we proposed a shrinking core model (SCM) which can be applicable to ALD on a porous monolith with tortuous pores.[23] In our SCM, it is assumed that the rate of consumption of the metal precursor by adsorption is approximately equal to the rate of the Knudsen diffusion of the precursor to the vacant sites on the moving boundary between the reacted (*i.e.*, chemisorbed) shell and unreacted (*i.e.*, unoccupied) core of the porous monolith. The minimum exposure time (τ_{cy}) of the precursor for a porous alumina monolith with a cylindrical shape is predicted to be $\tau_{cy} = \rho_{OH}R^2/4D_eC_o$ where ρ_{OH} is a molar volumetric density of OH groups, R is a radius of the monolithic cylinder, D_e is an effective diffusion coefficient of the precursor in porous alumina, and C_o is a concentration of the precursor on the exterior surface. In the previous report, the SCM was verified on a cylindrical

[a]These authors contributed equally to this work.

porous alumina monolith by ZnO ALD from diethylzinc (DEZ) and water.

Here we performed TiO_2 ALD by using $TiCl_4$ and water on the same porous alumina which had been used for ZnO ALD in the previous work. Because the byproduct HCl in TiO_2 ALD can chemically adsorb on the adsorption sites, while ethane (the byproduct of ZnO ALD) cannot occupy the adsorption sites, the SCM was modified in order to consider the chemisorption of the byproduct. The minimum exposure time and effective diffusion coefficient of $TiCl_4$ for TiO_2 ALD was determined by the modified SCM, and compared with ZnO ALD from DEZ and water.

Experimental

Length and diameter of the cylindrical alumina monoliths (cylindrical extrudate, Sasol) are 6.2 ± 2.0 mm and 1.93 ± 0.08 mm, respectively. The apparent density (ρ_M) of one alumina monolith is ~0.703 g/cm^3. Surface area (256 m^2/g), average pore diameter (8.9 nm) and pore volume (0.863 cm^3/g) of the monolithic cylinders are determined by Brunauer-Emmett-Teller and Barrett-Joyner-Halenda methods using an ASAP2020 Surface Area Analyzer (Micromeritics). The porosity (ε) was calculated to be 0.61 from the pore volume and the density of the porous alumina monoliths. The characteristics of the alumina monolith were summarized in Table 1.

TiO_2 ALD was performed only for 1 cycle on 10 g of the porous alumina (~790 ± 50 monoliths) at room temperature. When the alumina was loaded in ALD reactor, the height of the loaded monoliths was 5.5 ± 0.2 mm. The pulses of $TiCl_4$ and water were flowed from the bottom to the top of the loaded layer. $TiCl_4$ was supplied in a flow rate of 0.137 g/min (0.722 mmol/min) without any carrier gas, and water was carried in a flow rate of 0.078 g/min (4.33 mmol/min) by N_2 gas for 1.5 h. For the purging steps, excess $TiCl_4$ and byproducts were only evacuated without any purging gas for 2 h. For the water, the purging time was 15 h by evacuation. Therefore our ALD sequence can be summarized as: $TiCl_4$ exposure (variable times) - purge (2 h) - water exposure (1.5 h) - purge (15 h). The base pressure of our ALD system was ~6×10^{-2} torr, and the working pressures were 1.5-3.5 torr for $TiCl_4$ and 2.8-4.0 torr for water. All parts of our ALD system were maintained at room temperature during the ALD process.

TiO_2 growth behavior was investigated with the mass gain on alumina after the ALD process. Because the total surface area of 10 g of the alumina is around 2500 m^2, the mass gain due to TiO_2 growth can be measured by a digital balance even for 1 cycle. The penetration depth of TiO_2 from the exterior surface into the center in the circular cross-section of the cylinder was determined from energy-dispersive spectrometric (EDS) profile of titanium in field emission scanning electron microscope (FE-SEM).

Table 1. The characteristics of the porous alumina monolith

Length	6.2 ± 2.0 mm
Diameter	1.93 ± 0.08 mm
Apparent density (ρ_M)	0.703 g/cm^3
Surface area	256 m^2/g
Average pore diameter	8.9 nm
Average pore volume	0.863 cm^3/g
porosity (ε)	0.61

Results and Discussion

Figure 1 shows the mass gain (solid circles) on 10 g of cylindrical monoliths as a function of $TiCl_4$ exposure time. As the exposure time of $TiCl_4$ increases, the mass gain due to TiO_2 growth rapidly increases and subsequently saturates in ~15 min. In order to monitor the penetration depth of TiO_2 from the external surface of the cylindrical monolith, the cross-sectional area of the alumina cylinder was investigated for Ti peak by SEM-EDS as shown in Figure 2 and Figure S1 (See the Supplementary Materials). The open circles in Figure 1 show the penetration depth of TiO_2 in the cylindrical monolith of which the full depth from the external surface to the core is 0.97 mm. As the exposure time of $TiCl_4$ increases, the penetration depth also becomes deeper. The internal surface of the monolith was fully deposited by TiO_2 in the exposure time of ~15 min which is much shorter time comparing with the minimum exposure time of DEZ ($\tau_{cy,DEZ}$ ~ 66 min) on the same alumina monolith.[23] The rapid penetration of TiO_2 growth is originated from the chemisorption of the byproduct HCl which is accompanied by the chemisorption of $TiCl_4$ in the alumina monolith (*vide infra*).

In the generally accepted mechanism of TiO_2 growth, $TiCl_4$ mainly reacts with the surface OH groups releasing HCl in the first-half reaction:

$$n(\text{-OH})(s) + TiCl_4(g) \rightarrow (\text{-O-})_nTiCl_{4-n}(s) + nHCl(g) \quad (1)$$

where (s) denotes surface. The chlorotitanium species may react with water releasing HCl again in the second-half reaction:

$$(\text{-O-})_nTiCl_{4-n}(s) + (4-n)H_2O(g) \rightarrow (\text{-O-})_nTi(OH)_{4-n}(s) + (4-n)HCl(g) \quad (2)$$

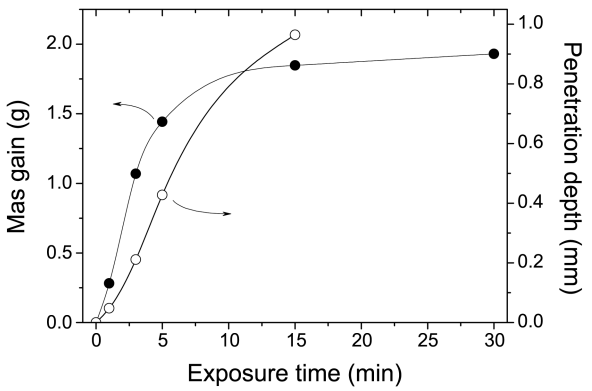

Figure 1. Mass gain (solid circle) by one ALD cycle on 10 g of cylindrical monoliths and penetration depth (open circle) of TiO_2 as a function of exposure time of $TiCl_4$.

In Eqs. (1) and (2), when n = 1 and n = 2, the reactions are monofunctional and bifunctional, respectively. According to the report by Ritala *et al.*,[24] the n shows a decreasing tendency as the ALD temperature increases (n ~ 2 at T = 150 °C; n ~ 1 at T = 250 °C; n < 1 at T > 250 °C). Because our ALD was performed at room temperature, it is believed that the first- and second-half reactions are bifunctional (n = 2). Thus the SCM equation for $TiCl_4$ exposure should be modified to consider the stoichiometry of the first-half reaction. In the Ref. 23, because the first-half reaction of ZnO ALD is monofunctional (n = 1), $-dN_{DEZ} = -dN_{OH}$ where N_{DEZ} and N_{OH} are the numbers of moles of DEZ molecules and hydroxyl groups, respectively. However, for the first half reaction of TiO_2 ALD, $-2dN_{TiCl_4} = -dN_{OH}$ where N_{TiCl_4} is the number of moles of $TiCl_4$, since two hydroxyl groups are consumed by one $TiCl_4$ molecule. Thus the equation of the SCM is modified with the stoichiometric coefficient n as below:

$$t = \frac{\rho_{OH}R^2}{4nD_eC_o}\left(1-\left(\frac{\xi}{R}\right)^2+\left(\frac{\xi}{R}\right)^2\ln\left(\frac{\xi}{R}\right)^2\right) \quad (3)$$

where t and ξ is the exposure time and the radius of the unreacted core, respectively. In our experimental conditions, R = 0.97 mm, and C_o is calculated to be ~1.45 × 10^{-7} mol/cm^3 from the working pressure of ~2.6 torr during the $TiCl_4$ exposure.

In the Ref. 23, The value of ρ_{OH} was calculated to be ~2.6 × 10^{-3} mol/cm^3 by using the reported areal density (d_{OH} = 8.7 OH/nm^2) of OH groups on alumina,[25,26] specific surface area (S = 256 m^2/g) and the density of the monolith (ρ_M = 0.703 g/cm^3):

$$\rho_{OH} = \frac{d_{OH}SW/N_A}{W/\rho_M} = \frac{d_{OH}\rho_M S}{N_A} \quad (4)$$

where W and N_A are the weight of the used monoliths (W = 10 g in this work) and the Avogadro's number, respectively. However it should be noted that all adsorption sites (*i.e.*, OH groups) cannot be completely occupied by the precursor molecules due to the molecular bulkiness, repulsive interaction between the chemisorbed molecules, and an undesirable occupation by byproduct (*e.g.* HCl). Especially, HCl released in the first- and second-half reactions may react with surface OH groups and/or oxygen bridges consuming the adsorption sites as shown in Eqs. (5)-(7).

$$(\text{-OH})(s) + HCl(g) \rightarrow (\text{-Cl})(s) + H_2O(g) \quad (5)$$

$$Ti(\text{-O-})_2Ti(s) + HCl(g) \rightarrow Ti(Cl)\text{-O-}Ti(OH)(s) \quad (6)$$

$$Ti(\text{-O-})_2Ti(s) + 2HCl(g) \rightarrow Ti(Cl)\text{-O-}Ti(Cl)(s) + H_2O(g) \quad (7)$$

Indeed, the ratio (C_{Ti}/C_{Cl}) of Ti to Cl atomic contents on the monolith exposed for 15 min was determined to be ~0.805 by EDS. Considering Ti occupies two adsorption sites (n = 2), the fraction of the adsorption sites occupied by Ti can be defined as

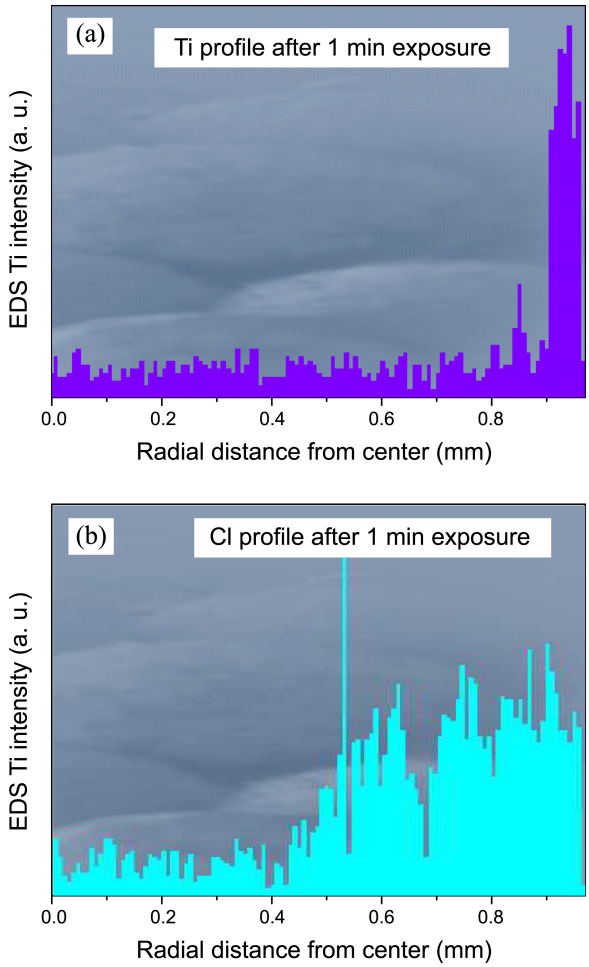

Figure 2. (a) EDS Ti and (b) Cl profiles in the circular cross-section of an 1 min-exposed monolith as a function of the radial distance from the center.

$$f_{Ti} = \frac{nC_{Ti}}{nC_{Ti}+C_{Cl}} \quad (8)$$

This reveals that 38.3% of the available adsorption sites are occupied by HCl instead of $TiCl_4$. Furthermore the adsorption of HCl takes place prior to that of $TiCl_4$ due to the lighter molecular weight of HCl, as compared with the monolith exposed for 1 min in Figure 2. Thus the adsorption of $TiCl_4$ can occur mainly on the remained among the available sites. Therefore, an effective areal density ($d_{e,OH}$) of OH groups, which actually contribute the chemisorption of the metal precursor, may be preferred to d_{OH}.

The effective areal density of OH groups, $d_{e,OH}$ can be approximated by the product of the stoichiometric coefficient (n) and the areal density (d_{layer}) of the layer (*e.g.*, TiO_2) grown by one ALD cycle:

$$d_{e,OH} \approx nd_{layer} = n\frac{\Delta m_L N_A}{SWM_L} = \frac{nm_s N_A}{SM_L} \quad (9)$$

where Δm_L and M_L are the mass gain by the layer growth in the full penetration and the molecular mass of the grown layer (*e.g.*, TiO_2), respectively. m_s is a specific mass gain

defined as $m_s = \Delta m_L/W$. The Δm_L is calculated to be ~1.188 g from the total mass gain (1.848 g) at the exposure of ~15 min by considering $C_{Ti}/C_{Cl} \sim 0.805$. Thus for the TiO_2 ALD, $d_{e,OH}$ for TiO_2 ALD is calculated to be ~6.8 OH/nm^2. Following the similar calculation, $d_{e,OH}$ for ZnO ALD from DEZ is evaluated to be ~8.7 OH/nm^2. Even though we have used the same porous monoliths for both ALDs, the values of $d_{e,OH}$ are significantly different due to the undesirable adsorption of the byproduct in TiO_2 ALD.

By replacing d_{OH} in Eq. 4 by $d_{e,OH}$ in Eq. (9), an effective volumetric density ($\rho_{e,OH}$) of OH groups can be expressed as:

$$\rho_{e,OH} = \frac{n m_s \rho_M}{M_L} \tag{10}$$

Substituting Eq. (10) to Eq. (3), we finally obtain the modified SCM equation for the exposure time:

$$t = \frac{\rho_{e,OH} R^2}{4 n D_e C_o}\left(1 - \left(\frac{\xi}{R}\right)^2 + \left(\frac{\xi}{R}\right)^2 \ln\left(\frac{\xi}{R}\right)^2\right) \tag{11}$$

The minimum exposure time (τ_{cy}) for the complete penetration into the core of the cylindrical monolith is given by taking $\xi = 0$ in Eq. (11),

$$\tau_{cy} = \frac{\rho_{e,OH} R^2}{4 n D_e C_o} = \frac{m_s \rho_M R^2}{4 D_e C_o M_L} \tag{12}$$

As shown in Eq. (12), the stoichiometry of the chemisorption does not influence on the minimum exposure time because n is disappeared by considering the effective volumetric density of OH groups.

Figure 3 shows the experimental data (open circles) of exposure times as a function of the radial distance from the center in the cylindrical monolith. In order to obtain D_e of the precursor on the monolith, the data except for $t = 15$ min were fitted by Eq. (11). Although the monolith was completely reacted by $TiCl_4$ at 15 min, the data cannot be used

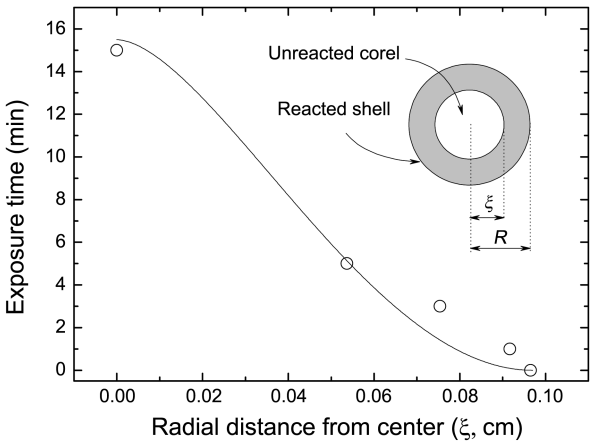

Figure 3. Experimental (solid circle) and SCM-predicting (solid line) exposure times of TiO_2 as a function of the radial distance from the center in the cylindrical monolith. The inset is a representation of a reacting cylindrical monolith during $TiCl_4$ exposure. R and ξ are the radii of the cylinder and the unreacted core, respectively.

for the non-linear regression since it is possible for the reaction to be early completed in a shorter time than 15 min. The fitted result was drawn as a solid line in Figure 3, and D_e was evaluated to be ~1.78×10^{-2} cm^2/s.

Similarly, the D_e value of DEZ was obtained to be ~1.3×10^{-2} cm^2/s by using the modified SCM. This is slightly smaller value than that (~1.4×10^{-2} cm^2/s) of Ref. 23 in which the effectiveness of the volumetric density of OH group was not considered. By using the fitted value of D_e in Eq. (12), the modified SCM predicts the minimum exposure times for DEZ and $TiCl_4$ are 71 and 16 min, respectively. These values well agree with the experimental values of DEZ (70 min) and $TiCl_4$ (15 min).

According to the kinetic theory of gases, the diffusion coefficient (D) of a gas with a molecular mass M is given by

$$D = \frac{1}{3}\lambda \bar{c} = \frac{\lambda}{3}\sqrt{\frac{8RT}{\pi M}} \tag{13}$$

where λ and $\bar{c}$ are the mean free path and mean speed of the gas, respectively.[27] In the Knudsen diffusion of a gas in a capillary with a diameter d_C, the mean free path can be approximated with d_C, because the gas molecule collides with the wall of the capillary rather than with other molecules due to the large Knudsen number (Kn = $\lambda/d_C >> 1$). Thus the Knudsen diffusion coefficient (D_K) of the gas in the capillary is given by

$$D_K = \frac{d_C}{3}\sqrt{\frac{8RT}{\pi M}} \tag{14}$$

Because the porous alumina is not well represented by a collection of straight cylindrical capillaries, the d_C of the capillary is generally replaced by an equivalent diameter (d_e) of pores obtained from experimental values of the specific surface area (S), porosity (ε) and apparent density (ρ_M)of the porous monolith.[28] The equivalent diameter (d_e) is simply the diameter of the pore when the alumina has the same surface-to-volume ratio with the capillary, *i.e.*, area of a capillary/volume of a capillary = $4/d_C$, and,

$$d_C = d_e = \frac{4\varepsilon}{S\rho_M} \tag{15}$$

Then the Knudsen diffusion coefficient is given by

$$D_K = \frac{d_e}{3}\sqrt{\frac{8RT}{\pi M}} = \frac{4\varepsilon}{3S\rho_M}\sqrt{\frac{8RT}{\pi M}} \tag{16}$$

By using Eq. (16), the Knudsen diffusion coefficients of DEZ and $TiCl_4$ are evaluated to be ~1.02×10^{-2} and ~8.27×10^{-3} cm^2/s, respectively. It should be noted that the Knudsen diffusion model predicts a smaller D_K value for $TiCl_4$ than D_K of DEZ due to its heavier molecular mass. However the non-linear regression by using the modified SCM gives significantly larger D_e value for $TiCl_4$ than D_e of DEZ. This discrepancy may be originated from the desorption of the chemisorbed chlorotitanium species through the reverse reaction of Eq. (1). Recently, Hu and Turner theoretically

investigated the possibility of the reverse reaction.[30] The desorption may result in the overestimation of D_e because of the increase in the flux of $TiCl_4$ on the moving boundary between the reacted shell and unreacted core.

Conclusions

ALD of TiO_2 on a porous alumina with ultrahigh aspect ratio is limited by Knudsen diffusion of $TiCl_4$ within the pores. Because all adsorption sites cannot be completely occupied by the precursor molecules due to the undesirable occupation by the byproduct (*i.e.*, HCl), the SCM was modified in order to consider the effective areal density of OH groups which were actually occupied by $TiCl_4$. The effective density of OH groups for $TiCl_4$ is evaluated to be ~6.8 OH/nm^2 which is significantly smaller value in comparison to DEZ (~8.7 OH/nm^2) due to the adsorption of the byproduct. By fitting the experimental data with the modified SCM, the effective diffusion coefficient of $TiCl_4$ and DEZ were 1.78×10^{-2} and 1.3×10^{-2} cm^2/s, respectively. The modified SCM predicts that the minimum exposure times for $TiCl_4$ and DEZ were 16 and 71 min, respectively, which well agreed with the observed values.

Acknowledgments. This paper was supported by Konkuk University in 2010.

Supplementary Materials. EDS profiles of Ti for the monoliths exposed by $TiCl_4$ for 3, 5 and 15 min, respectively.

References

1. Suntola, T.; Antson, J. *US Patent* **1977**, 4,058,430.
2. Suntola, T. *Thin Solid Films* **1992**, *216*, 84.
3. Suntola, T., In *Handbook of Crystal Growth*; Hurle, D. T. J., Ed.; Elsevier: Amsterdam, **1994**; Vol. 3, Chapter 14.
4. Ritala, M.; Leskela, M. *Nanotechnology* **1999**, *10*, 19.
5. Ritala, M.; Leskela, M. In *Handbook of Thin Film Materials*; Nalwa, H. S., Ed.; Academic Press: San Diego **2002**, Vol. 1, Chapter 2.
6. Leskela, M.; Ritala, M. *Angew. Chem. Int. Ed.* **2003**, *42*, 5548.
7. George, S. M. *Chem. Rev.* **2010**, *110*, 111.
8. Lindblad, M.; Lindfors, L. P.; Suntola, T. *Catal. Lett.* **1994**, *27*, 323.
9. Rautiainen, A.; Lindblad, M.; Backman, L. B.; Puurunen, R. L. *Phys. Chem. Chem. Phys.* **2002**, *4*, 2466.
10. Min, Y. S.; Bae, E. J.; Jeong, K. S.; Cho, Y. J.; Lee, J. H.; Choi, W. B. *Adv. Mater.* **2003**, *15*, 1019.
11. Min, Y. S.; Bae, E. J.; Song, J.; Park, J. B.; Park, N. J.; Park, W.; Hwang, C. S. *Appl. Phys. Lett.* **2007**, *90*, 263104.
12. Min, Y. S.; Lee, I. H.; Lee, Y. H.; Hwang, C. S. *CrystEngComm*. **2011**, *13*, 3451.
13. Gordon, R. G.; Hausmann, D.; Kim, E.; Shepard, J. *Chem. Vap. Deposition* **2003**, *9*, 73.
14. Elam, J. W.; Routkevitch, D.; Mardilovich, P. P.; George, S. M. *Chem. Mater.* **2003**, *15*, 3507.
15. Kucheyev, S. O.; Biener, J.; Wang, Y. M.; Baumann, T. F.; Wu, K. J.; van Buuren, T.; Hamza, A. V.; Satcher, J. H., Jr.; Elam, J. W.; Pellin, M. J. *Appl. Phys. Lett.* **2005**, *86*, 083108.
16. Baumann, T. F.; Biener, J.; Wang, Y. M.; Kucheyev, S. O.; Nelson, E. J.; Satcher, J. H., Jr.; Elam, J. W.; Pellin, M. J.; Hamza, A. V. *Chem. Mater.* **2006**. *18*, 6106.
17. Elam, J. W.; Libera, J. A.; Pellin, M. J.; Zinovev, A. V.; Greene, J. P.; Nolen, J. A. *Appl. Phys. Lett.* **2006**, *89*, 053124.
18. Elam, J. W.; Libera, J. A.; Pellin, M. J.; Stair, P. C. *Appl. Phys. Lett.* **2007**, *91*, 243105.
19. Biener, J.; Theodore, F. B.; Wang, Y.; Nelson, E. J.; Kucheyev, S. O.; Hamza, A.; Kemell, M.; Ritala, M.; Leskela, M. *Nanotechnology* **2007**, *18*, 055303.
20. Libera, J. A.; Elam, J. W.; Pellin, M. J. *Thin Solid Films* **2008**, *516*, 6158.
21. Kucheyev, S. O.; Biener J.; Baumann, T. F.; Wang, Y. M.; Hamza, A. V.; Li, Z.; Lee, D. K.; Gordon, R. G. *Langmuir* **2008**, *24*, 943.
22. Kim, J. Y.; Kim, J. H.; Ahn, J. H.; Park, P. K.; Kang, S. W. *J. Electrochem. Soc.* **2007**, *154*, H1008.
23. Lee, H. Y.; An, C. J.; Piao, S. J.; Ahn, D. Y.; Kim, M. T.; Min, Y. S. *J. Phys. Chem. C* **2010**, *114*, 18601.
24. Marero, R.; Rahtu, A.; Ritala, M. *Chem. Mater.* **2001**, *13*, 4506.
25. Kummert, R. In *Ph.D. Thesis*; Swiss Fedral Institute of Technology; Zurich, 1979.
26. Puurunen, R. L.; Lindblad, M.; Root, A.; Krause, A. O. I. *Phys. Chem. Chem. Phys.* **2001**, *3*, 1093.
27. Atkins, P.; De Paula, J., In *Physical Chemistry*, 8th Ed; Oxford University Press; Oxford, 2006; p 759.
28. Petersen, E. E. In *Chemical Reaction Analysis*; Prentice-Hall: New Jersey, 1965; p 115.
29. Forgler, H. S. In *Elements of Chemical Reaction Engineering*, 4th Ed; Pearson; New Jersey, 2006; p 815.
30. Hu, Z.; Turner, C. H. *J. Phys. Chem. B* **2006**, *110*, 8337.